XLIII CILAMCE
21-25, November, 2022
FOZ DO IGUAÇU - PR - BRAZIL

Analysis of temperature treatments and manufacture methods of superelastic niti bending springs with complex-shape

Sena I. J.[1], Senko R.[2]

[1]*Academic Unit of Mechanic Engineering, Federal University of Campina Grande*
igor.jordan@estudante.ufcg.edu.br
[2]*Academic Unit of Production Engineering, Federal University of Campina Grande*
richard.senko@ufcg.edu.br

Abstract. The application of smart materials in mechanical systems has been increasing, due to these materials presenting a capacity to reduce undesirable vibrations with a small increase of mass in the system. The most applied material is the Shape Memory Alloys (SMA), which change their characteristics with variations in temperature or mechanical stress. SMAs have two effects: shape memory effect (SME); which changes its phase with temperature variation, and superelasticity (SE); which modifies its phase with the change in mechanical stress. For the SMA-SE, properties such as damping capacity and complex stiffness are relevant for application in systems with undesirable vibrations, principally considering some external parameters such as temperature, frequency, and amplitude can change the properties of the material. However, if the SMA-SE device has a complex shape, more procedures are needed to achieve it. Thus, complex-shaped devices tend to be more liable to changes in the starting properties of the material during the process of obtaining the sought shape, due to the forming process. Therefore, focusing on obtaining balanced properties, such as damping capacity, complex stiffness, and transformation temperatures on the SMA-SE devices, several parameters should be considered during the manufacturing, such as time and temperature of the treatment, cooling speed, and the method of material forming. This paper aims to evaluate types of heat treatments, application of mechanical forming, and different types of cooling applied in the manufacture of superelastic NiTi bending springs with complex-shape, to obtain balanced properties for application in the rotating system to intend to reduce vibration in a passive form.

Keywords: Shape memory alloys, superelasticity, mechanical vibrations

1 Introduction

The increase application and studies related to shape memory alloys is due to the ability to recover the original shape when they are subjected to a variation in temperature or mechanical stress. This capacity is due to the crystalline structure of the material which, depending on the phase, martensitic or austenitic, has different effects such as shape memory effect (SME) and superelasticity (SE). SME occurs with the material fully in the martensitic phase and undergoing changes in the material's crystalline structure, when subjected to variations in temperature and stress. While the SE effect occurs above the austenite final temperature (Af) from the application of a mechanical stress on the material, which can generate an elastic deformation up to 8% in NiTi alloys and also a phase transformation to stress-induced martensite. This behavior is influenced by factors such as chemical composition of the material, cold work, heat treatments, among others. One of the applications of the LMF-SE is in rotating systems to reduce undesirable vibrations, this is due to the lack of need to use an external source of energy, as the material undergoes transformations through mechanical stresses arising from the system itself. However, there is a need to obtain better properties of this material, such as mechanical strength, adequate phase transformation temperatures, damping capacity, among others. These properties are important to improve the efficiency of the application of this material, since these studies found high temperatures of phase transformation of Af and low resistance to fatigue. This research aims to analyze and apply Heat Treatments, mechanical forming processes and manufacturing methods (shape setting) in C-shaped LMF-SE leaf springs, seeking to obtain balanced material properties to reduce mechanical vibrations.

2 Material and methods/Methodology

2.1 Manufacture of the LMF-SE type spring

In the manufacturing process of the C-shaped springs, Figure 1, it started with the cuts in the NiTi plate, with 55.8% nickel by weight, in the EDM machine, cutting samples with a length of 64 mm, width of 5 mm and thickness of 0.52 mm.

Figure 1 – C shaped type spring

After cutting the samples, heat treatment (HT) was applied for homogenization and stress relief (SOUZA) [1], for 10 minutes at a temperature of 450°C, as indicated by the manufacturer. After the common treatments for all the samples, these were separated according to the type of cooling and process applied, Figure 2.

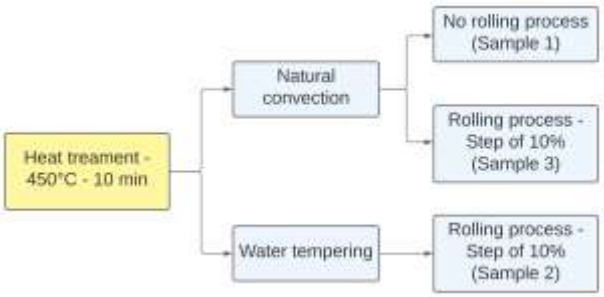

Figure 2 - Manufacturing flowchart

For sample 1, was selected the natural convection cooling process, to obtain a low temperature Af, based on the studies by HEIDARI, KADKHODAEI, et al., (2016) [2], and no rolling process was performed, keeping the initial thickness of 0.52 millimeters. Samples 2 and 3 had two types of cooling, natural convection and water quenching, and to increase the mechanical strength, both were subjected to the rolling process, as indicated by SASHIHARA, (2007) [3].

For the rolling process, two steps were performed to reduce the thickness of the bending spring by 10%. After each step, a HT was performed to relieve the internal stresses of the samples, at a temperature of 450°C for 20 minutes, resulting in a final thickness of 0.43 mm due to recrystallization. These procedures were the same performed by SENKO et al. (2022) [4] with M-shaped springs.

Finally, to obtain the C shape (Figure 1), the shape setting was performed using a carbon steel mold, composed of three pieces joined by bolts, Figure 3(A). After inserting the sample into the mold, a HT was performed at a temperature of 500°C for 30 minutes, followed by cooling by natural convection. These shape configuration parameters are suggested by RAO, SRINIVASA, et al., (2015) [5]. At the end of the shape setting, were obtained the C-shaped bending springs,Figure 3(B).

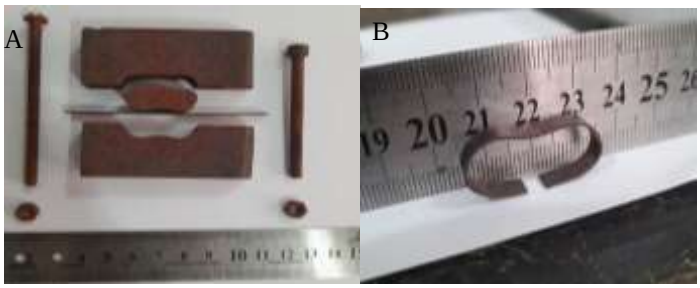

Figure 3 – (A) Carbon steel mold, (B) C-shaped bending spring

2.2 Characterization of the LMF-SE type spring

To obtain the phase transformation temperatures of the C-shaped LMF SE springs, the variation of electrical resistance as a function of temperature (RET) was performed. This technique consists of the controlled variation of the temperature of the sample, with the simultaneous monitoring of temperature and electrical resistance, making it possible to obtain the experimental curve electrical resistance versus temperature (DOS REIS, 2010) [6].

For mechanical characterization of NiTi alloys, we must follow the standard for wire tensile tests, ASTM F2516.26200 (2014). The specimens, Figure 4, used are produced by cutting LMF alloy sheets by electro-erosion.

Figure 4 - Tensile test specimen

This procedure was also performed by ALMEIDA (2020) [7], where a loading up to 6% strain was inserted, followed by unloading to a stress lower than 7 MPa, and loading until fracture. This is performed on the Instron® 5582 56 tensile testing machine, with video strain gauge (AVE) at room temperature ($\cong 22\ ^{o}CC$) and strain rate of 0.02 mm/min.

The determination of the material damping factor is performed by the System for Estimation of Material Damping (SEMD), presented by DOS REIS, R.P.B., SILVA, et al., (2019) [8], which is a modal analysis of 1 GDL to determine the loss factor and stiffness of the device.

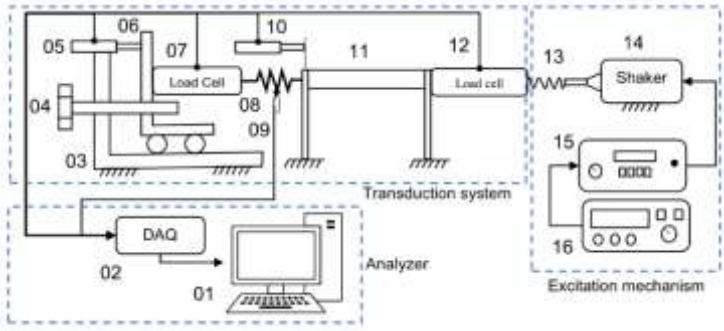

01 - Computer
02 - QUANTUM X ® model MX840A
03 – Aluminum support
04 - Offset positioning screw
05 -Linear displacement sensor (HBM model w/10mm)
06 - Linear displacement trolley
07 – Load cell (HBM model S2M/200N)
08 – Clamp for SMA -SE mini-springs
09 – K-type thermocouples
10 - Linear displacement sensor (HBM model w/10mm)
11 - SDOF system
12 - Load cell (HBM model U9C/50N)
13 - Stinger springs
14 - Shaker (modal shop model 2025E)
15 - Signal amplifier (modal shop model 2100E21-400 SMARTAMP™)
16 – Signal generator (KEYSIGHT model 33220A)

Figure 7 - SEMD

In this experiment, Figure 7, a displacement is applied, using the shaker (item 14), directly in the SDOF (Single Degree of Freedom) system (item 11), which has 1.485 kg, without the SMA-SE device. Following, the C-shape device (item 8) was placed in the position presented in Figure 7, and the same procedure was applied. The difference between the damping of the SDOF system with and without the SMA SE device under test, provides an estimate of the material damping, through the experimental FRF receptance curves, and Nyquist diagram. All details about the procedure of the SEMD are presented in the literature DOS REIS, R.P.B., SILVA, et al., (2019) [8].

3 Results and discussions

3.1 Transformation Temperatures

Figure 8 represents the curve obtained in the RET test for sample 1 and Table 1 presents all the results obtained.

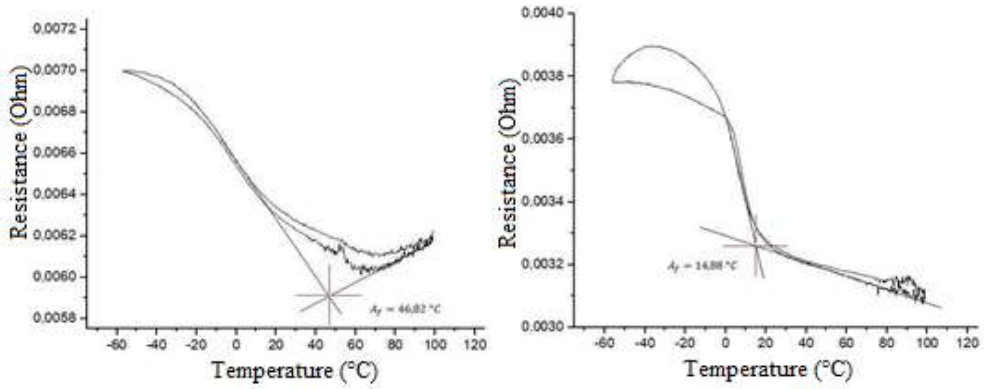

Figure 8 – Resistance Curve vs. Temperature

Table 1 – Samples Af Temperatures

RET	Sample 1	Sample 2	Sample 3
Af before manufacturing	46,82 °C	49,81 °C	28,67 °C
A_f after manufacturing	14,88 °C	21,12 °C	16,86 °C

.

For sample 1, before fabrication, a temperature Af of 46.82 °C was obtained, a value above the local ambient temperature (≅22 °C), which it is not desired for this application. On the other hand, after performing the shape setting, the temperature Af was reduced to 14.88°C. Therefore, the material tends to be completely in the austenitic phase at room temperature to take advantage of the full superelasticity effect, Patoor et al. (2006) [9].

In sample 2, the temperature Af was 49.81°C, a value above ambient temperature (≅22°C), after the shape setting, it decreased to 21.12 °C. Therefore, the material tends to be completely in the austenitic phase at room temperature. When compared with the results of ALMEIDA (2020) [7], the values differ, which obtained a temperature Af of 14.10 °C. However, was expected that this temperature would increase due to rolling process, as in SENKO et al. (2022) [4], where an increase in the phase transformation temperature happened due to this process.

As a result, in sample 3, a temperature Af of 28.67 °C was obtained, which was expected, considering that SENKO et al. (2022) [4] used the same heat treatment and the rolling process reached a temperature Af of 30.39 °C before shape setting. After the procedure, the temperature of Af of sample 3 obtained was 16.86 °C, ensuring that the material must be completely in the austenitic phase at room temperature.

According to Table 1, it can be seen that all the Af temperatures of samples after the shape setting were lower than the ambient temperature (≅22 °C), causing the material to be in the fully austenitic phase. The samples that

were rolled had a higher temperature Af due to the influence of rolling, as already reported.

3.2 Mechanical characterization of LMF NiTi sheets

Figure 9 shows the tensile test curve of sample 1 and Table 2 contains the results obtained for each sample. The austenitic Young's modulus greater than the martensitic was already expected, since the stiffness of the austenite phase is about four times greater than the martensite. The Failure Limit of Sample 1 was 1285.229 MPa, expected result due to cooling by natural convection, the same applied by SENKO (2018) [10], who obtained a rupture limit around 1200 MPa. The difference between the threshold stress (UPS and LPS) indicate around 44% of the UPS value, representing a high hysteresis area, so there is a high damping potential. The residual elongation of 0.0944% of the sample was low, indicating that few cycles are needed to achieve stabilization of the elastic behavior.

For Sample 2, the austenitic Young's modulus was also higjer than the martensitic. In addition, there was a high level of mechanical strength, with a tensile strength of 1429.61 MPa, corroborating SASHIRARA (2007) [3] and SENKO et al. (2022) [4], who applied rolling to increase mechanical strength. The residual elongation was 0.223%, being higher than when compared to the results of ALMEIDA (2020) [7], this means that more cycles will be needed to achieve the stabilization of the superelastic behavior. The difference between the threshold stress (UPS and LPS) represents around 38% of the UPS value, indicating a good potential for damping.

And for sample 3, the austenitic Young's modulus was higher than the martensitic, as was the case with the previous samples. In addition, a failure stress of 1476.66 MPa was obtained. This was due to natural convection cooling, which tends not to weaken the material, and rolling process, which according to SASHIRARA (2007) [3] increases the mechanical strength. Residual elongation was 0.114%, being lower than that obtained in the results of ALMEIDA (2020) [7]. The difference between the threshold stress (UPS and LPS) represents around 40% of the UPS value, symbolizing that the hysteresis area is relatively high, with a high damping potential.

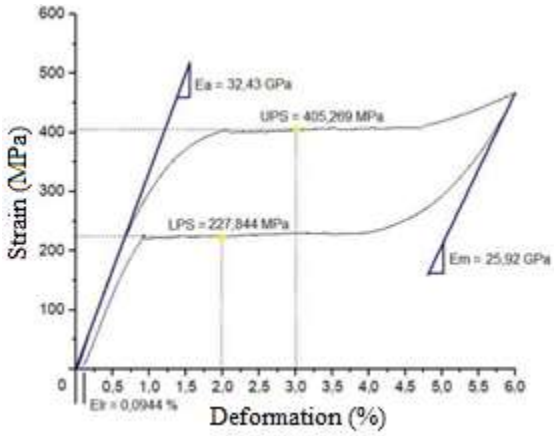

Figure 9 - Tensile test curve

Table 2 - Properties Obtained in the Tensile Test

	Ea (GPa)	Em (GPa)	UPS (MPa)	LPS (MPa)	Elr (%)	σrup (MPa)
Sample 1	32,43	25,92	405,269	227,844	0,0944	1285,23
Sample 2	27,96	23,71	452,971	281,155	0,223	1429,61
Sample 3	37,96	25,09	474,703	285,569	0,114	1476,66

3.3 Material damping

Through this experiment, the Nyquist diagram and the FRF of the three springs were obtained with the application of a preload of 1 mm, in which it was possible to obtain the loss factor ($\boldsymbol{\eta}$) of the samples and the hysteretic damping.

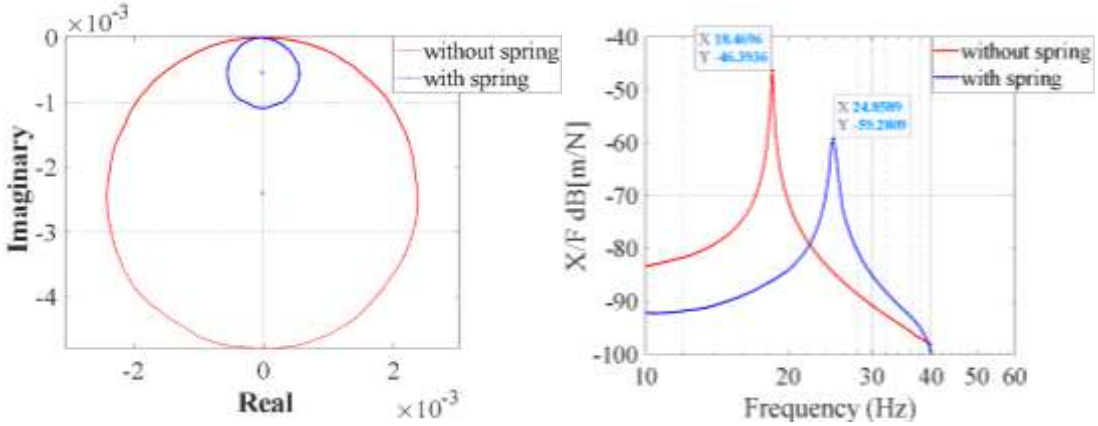

Figure 10 (A) Spring 1 Nyquist Diagram, (B) Spring 1 FRF

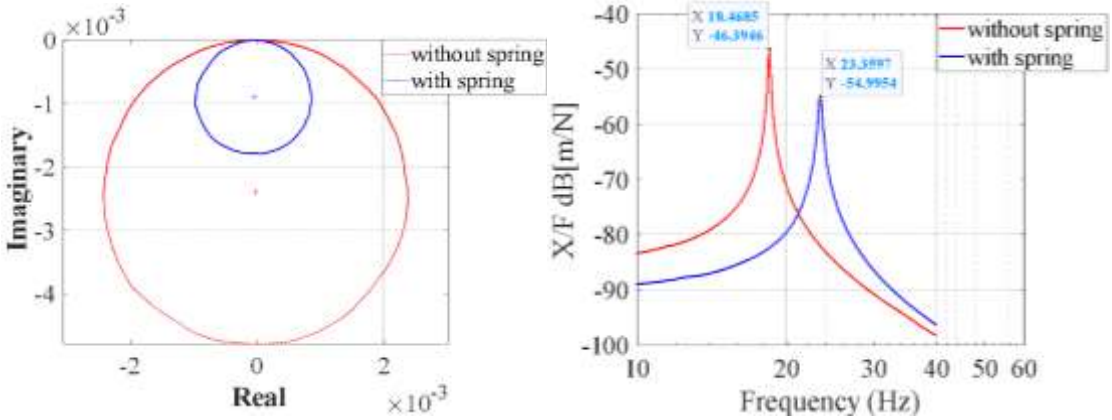

Figura 11 (A) Spring 2 Nyquist Diagram, (B) Spring 2 FRF

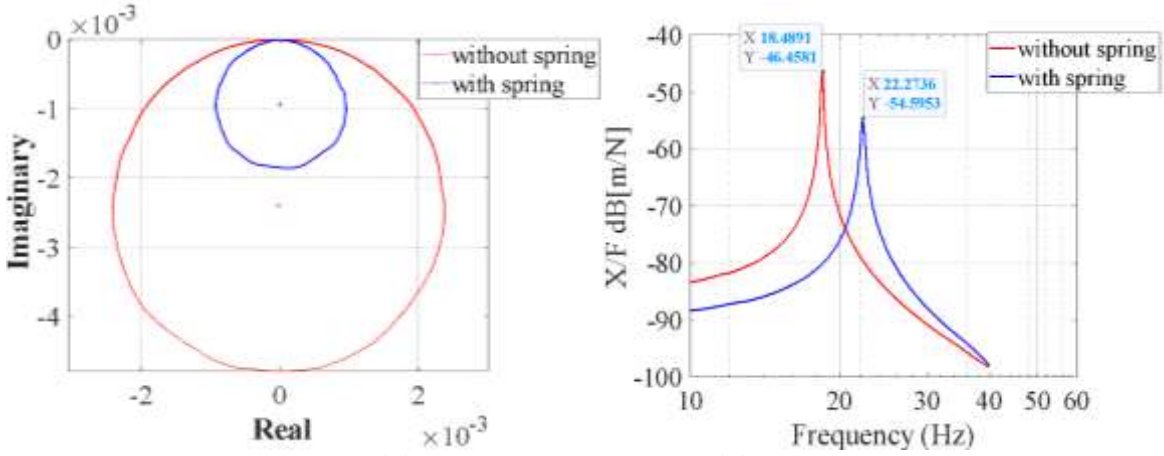

Figura 12 (A) Spring 3 Nyquist Diagram, (B) Spring 3 FRF

In all samples it is possible to notice the reduction of the Nyquist circle in the system when the spring is inserted, indicating the high damping potential of the device.

The hysteretic damping of the system without the spring is 208.4249 N/m and with spring 1 this value increased to 718.8263 N/m, which resulted in an increase of 71.00%, in which a loss factor of 4.66%. In FRF, a reduction of 12.9479 dB in amplitude is observed in the system with spring, compared to the system without.

Meanwhile, when spring 2 was inserted into the system, , the value of hysteretic damping obtained was

347.1868 N/m, resulting in an increase of 39.97%, with a damping factor of 3.04% and a reduction of 8.3358 dB in system amplitude.

Finally, when spring 3 was inserted into the system, the hysteretic damping achieved was 332.6668 N/m, which resulted in an increase of 37.35%, with a loss factor of 3.90%. In FRF, there is an 8.2017 dB reduction in system amplitude.

4 Conclusions

With the application of heat treatments and the rolling process in the manufacture of three types of complex-shaped springs, a temperature Af below ambient was obtained, which is considered ideal, as it will not be necessary to use an external source or expect the self-heating as occurred in [4]. While with the mechanical characterization it was demonstrated that samples 2 and 3 that were laminated, obtained a greater mechanical resistance when compared to sample 1, corroborating the studies of [3]. However, sample 1 still has a mechanical strength twice as high as the results of [7]. On the other hand, sample 1, which did not have the thickness changed and cooled slowly in air, obtained a greater loss factor and hysteretic damping, corroborating studies by [11] and [10]. Therefore, the spring that has the best balance of properties to be applied as a vibration attenuator is sample 1.

References

[1] SOUZA, E. F. De. **Experimental Study of the Thermal and Dynamic Behavior of a Belleville Spring with NiTi Shape Memory Alloy**. 2015. 26 f. Federal University of Campina Grande, 2015.

[2] HEIDARI, B., KADKHODAEI, M., BARATI, M., *et al.* "Fabrication and modeling of shape memory alloy springs", **Smart Materials and Structures**, v. 25, n. 12, 10 nov. 2016. DOI: 10.1088/0964-1726/25/12/125003.

[3] SASHIHARA, E. M. **Production of Ni-Ti alloy with shape memory effect in an electronic beam melting furnace and its characterization**. 2007. 134 f. Technological Institute of Aeronautics (ITA), 2007

[4] Senko R, Almeida VS, Dos Reis RPB, Oliveira AG, Silva AA, Rodrigues MC, de Carvalho LH, Lima AGB. Passive Attenuation of Mechanical Vibrations with a Superelastic SMA Bending Springs: An Experimental Investigation. Sensors (Basel). 2022 Apr 21;22(9):3195. doi: 10.3390/s22093195. PMID: 35590893; PMCID: PMC9103138.

[5] RAO, A., SRINIVASA, A. R., REDDY, J. N. **Design of Shape Memory Alloy (SMA) Actuators**. Cham, Springer International Publishing, 2015. Available in: http://link.springer.com/10.1007/978-3-319-03188-0. (SpringerBriefs in Applied Sciences and Technology).

[6] DOS REIS, Rômulo Pierre Batista. **Development of an equipment for thermal characterization of shape memory alloy actuators using thermoelectric effect**. 2010. 58 f. Federal University of Campina Grande, 2010.

[7] ALMEIDA, V. S. Development and Tests of Vibration Attenuation in Rotating System Bearings Applying Shape Memory Alloy Blade Actuators in the Superelastic Regime. 2020 (Master's Thesis). Academic Unit of Mechanical Engineering, Federal University of Campina Grande

[8] DOS REIS, Rômulo Pierre Batista. **Effect of the incorporation of superelastic NiTi minisprings on structural damping: applications in passive attenuation of wind turbine blades**. 2018. 123 f. UFCG, 2018

[9] PATOOR, E., LAGOUDAS, D. C., ENTCHEV, P. B., *et al.* "Shape memory alloys, Part I: General properties and modeling of single crystals", **Mechanics of Materials**, v. 38, n. 5–6, p. 391–429, maio 2006. DOI: 10.1016/j.mechmat.2005.05.027. Available in: https://linkinghub.elsevier.com/retrieve/pii/S0167663605001195.

[10] SENKO, R. **Passive attenuation of a rotating system using superelastic blades of SMA**. 2018. 177 f. Federal University of Paraíba, 2018. DOI: https://repositorio.ufpb.br/jspui/handle/123456789/12967. Available in: https://repositorio.ufpb.br/jspui/handle/123456789/12967.

[11] MOTEMANI, Y., NILI-AHMADABADI, M., TAN, M. J., *et al.* "Effect of cooling rate on the phase transformation behavior and mechanical properties of Ni-rich NiTi shape memory alloy", **Journal of Alloys and Compounds**, v. 469, n. 1–2, p. 164–168, fev. 2009. DOI: 10.1016/j.jallcom.2008.01.153. Available in: https://linkinghub.elsevier.com/retrieve/pii/S0925838808002120.